

*Full Length Research Paper*

# An experimental study on shear reinforcement in RC beams using CFRP-bars

Mohsen Kobraei\*, Mohd Zamin Jumaat and Payam Shafigh

Department of Civil Engineering, Faculty of Engineering, University of Malaya,  
50603 Kuala Lumpur, Malaysia.

Accepted 13 July, 2011

**Fibre reinforced polymer (FRP) as an alternative to steel in reinforced concrete (RC) beams has become increasingly popular. The merits of FRP include high strength to weight ratio and corrosion resistance, and its advantages cannot be ignored in civil engineering. Consequently, FRP has attracted considerable interest from researchers. In this research, the effects of using CFRP bars as shear reinforcement instead of stirrups in RC beams have been investigated. All beams were cast using a high strength concrete (HSC), which was also a self-compacting concrete (SCC). For this new idea, modes of failure for seven laboratory specimens, including a comparison of the ultimate moment capacity of beams, load-deflection control, load of first crack, crack width and position of the neutral axis (N.A.) were analysed. The results show that using carbon fibre reinforced polymer (CFRP) shear reinforcement can be an acceptable alternative for normal stirrups in RC beams.**

**Key words:** Concrete beam, fibre reinforced polymer, flexural behaviour, ultimate moment, deflection, shear behaviour, first crack, neutral axis.

## INTRODUCTION

FRP composites are the most modern version of the very old idea of making better composite materials by combining two different materials (AIMusallam et al., 1997; Alsayed, 1998) which can be traced back to the use of straw as reinforcement in bricks used by ancient civilizations (for example Egyptians in 800). The mechanical properties of FRP bars are usually considerably different from those of steel bars and mainly depend on both the matrix and the type of fibre as well as on their volume fraction. However, in general, FRP bars have lower weight, lower Young's modulus but higher strength than steel (Thériault and Benmokrane, 1998; Tureyen and Frosch, 2002; Yost et al., 2001). The most commonly available types of fibre are carbon (CFRP), glass (GFRP) and aramid (AFRP) (ACI 440, 2006). Table 1 lists some of the advantages and disadvantages of FRP reinforcement for concrete structures when compared with conventional steel reinforcement as

reported by ACI 440.1R-06. The determination of both the geometrical and mechanical properties of FRP bars requires the use of specific procedures (ASTM D 618, ACI 440.3R-04). FRP bars have densities ranging from one fifth to one fourth that of steel; the reduced weight eases the handling of FRP bars on the project site (ACI Committee 440, 2006). The tensile properties of FRP are what make them an attractive alternative to steel reinforcement. When loaded in tension, FRP bars do not exhibit any plastic behaviour (yielding) before rupture. Table 2 gives the most common tensile properties of reinforcing bars in compliance with the values reported by ACI 440.1R-06. Figure 1 depicts the typical stress-strain behaviour of FRP bars compared to that of steel bars. Near-surface mounted (NSM) is a recent and promising method for shear strengthening of reinforced concrete (RC) members using fibre-reinforced polymer (FRP) reinforcement (Rizzo and Lorenzis, 2007). NSM is based on the use of circular (Lorenzis and Nanni, 2002) or rectangular cross sectional bars (Blaschko and Zilch, 1999) of carbon or glass fibre reinforced polymer (CFRP or GFRP) installed into pre-cut slits in the concrete cover of the elements to be strengthened. NSM requires no

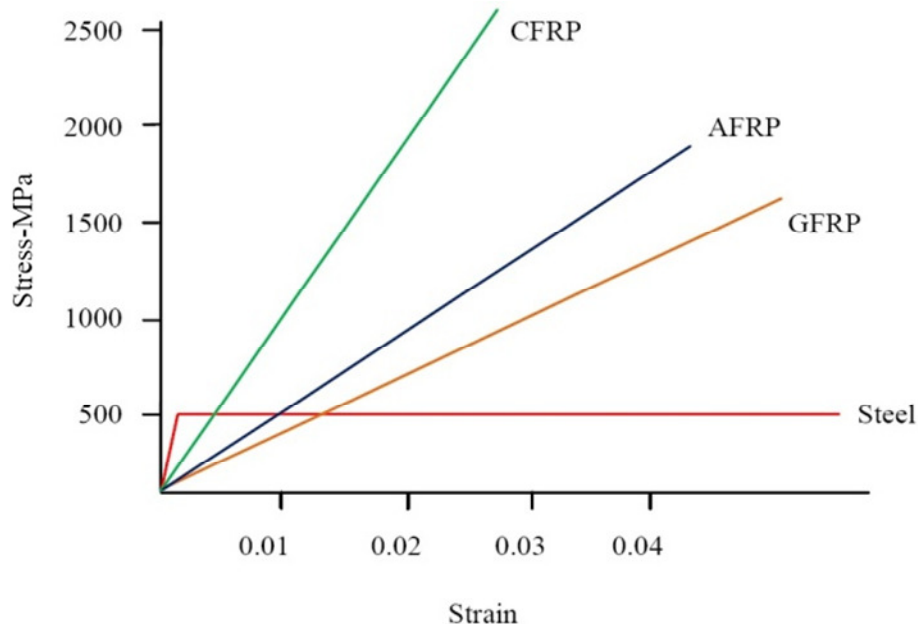
\*Corresponding author. E-mail: mkobraei@yahoo.com Tel: +60 12 668 7348.

**Table 1.** Advantages and disadvantages of FRP (ACI 440, 2006).

Advantages of FRP reinforcement	Disadvantages of FRP reinforcement
High longitudinal tensile strength	No yielding before brittle rupture.
Corrosion resistance	Low transverse strength.
Nonmagnetic	Low modulus of elasticity.
High fatigue endurance	Susceptibility of damage to polymeric resins and fibres under ultra violet radiation exposure.
Light weight (about 1/5 to 1/4 the density of steel)	High coefficient of thermal expansion perpendicular to the fibres, relative to concrete.
Low thermal and electric conductivity	May be sensitive to fire depending on matrix type and concrete cover thickness.

**Table 2.** Typical tensile properties of FRP (ACI 440, 2006).

	Steel	GFRP	CFRP	AFRP
Nominal yield stress (MPa)	276 to 517	N/A	N/A	N/A
Tensile strength (MPa)	483 to 690	483 to 1600	600 to 3690	1720 to 2540
Elastic modulus (GPa)	200	35 to 51	120 to 580	41 to 125
Yield strain (%)	0.14 to 0.25	N/A	N/A	N/A
Rupture strain (%)	6.0 to 12.0	1.2 to 3.1	0.5 to 1.7	1.9 to 4.4

**Figure 1.** Stress-strain curves of typical reinforcing bars (ACI 440, 2006).

surface preparation work and, after cutting the slit, requires minimal installation time compared to the externally bonded reinforcing (EBR) technique.

A further advantage associated with NSM is its ability to significantly reduce the probability of harm resulting from acts of vandalism, mechanical damage and the effects of aging. When NSM is used, the appearance of a structural element is practically unaffected by the strengthening intervention. Since both faces of the laminate are bonded to concrete when using CFRP laminates, high strengthening efficacy has been attributed to the NSM

technique for both flexural (Barros and Fortes, 2005; El-Hacha and Rizkalla, 2004; Wang et al., 2009; Ali et al., 2008; Badawi and Soudki, 2009) and shear strengthening (Islam, 2009; Novidis et al., 2007; Yang and Wu, 2007) of concrete structures. The idea of this research comes from the near-surface mounted (NSM) method. It is investigated the usage of CFRP-bars used as shear reinforcement in concrete beams at the time of casting the concrete, not after casting or for subsequent strengthening. To manufacture a beam according to the usual method, normal stirrups in the areas of shear is



**Figure 2.** Sand-coated CFRP bars and its failure shape.

**Table 3.** Details of used CFRP.

Nominal diameter (mm)	Tensile strength (MPa)	Modulus of elasticity (GPa)	Carbon fibre linear weight (g/mm <sup>2</sup> )	Density (g/cm <sup>3</sup> )	Normal area (mm <sup>2</sup> )
12	2400	200	195	1.65	113

used. Of course, to build a beam using the usual method requires time to bend the bars and make the stirrups. However, if being used straight bars as shear reinforcement, it is possible to make more beams in a certain time. As commonly known, problems occur in placing the reinforcement when building concrete beams in huge structures; therefore, it is impossible to do it well particularly at the junctions of beams and columns. Hence, it would be helpful to reduce the reinforcement bars without reducing the strength of the beams. This study has never been done before and is a new idea that offers a new method to build RC beams.

#### EXPERIMENTAL PROGRAMME

The experimental programme consisted of seven RC beams. The RC beams were divided into two groups: group one were strengthened using steel and CFRP longitudinal reinforcement of 12 mm diameter; and group two were strengthened by steel bars of 14 mm diameter. One beam in group one was used as the control

beam with normal stirrups and straight shear reinforcement was used in five beams comprising CFRP-bars and steel bars.

#### Properties of materials

Three materials were used in this study. These materials were CFRP, steel bars and concrete. Subsequently, the characteristics of the materials used in this study are as follows:

##### CFRP bars

The data sheet provided by the manufacturer shows that the modulus of elasticity is 200 GPa. The CFRP exhibits a linear elastic behaviour up to failure. Therefore, the ultimate strength of the CFRP rod based on the failure strain would be about 2400 MPa. It has a high strength and a high modulus. Pre-fabricated carbon FRP (12 mm diameter) was used as shear and longitudinal reinforcement for the beam specimens. The CFRP bars had a sand-coated surface as shown in Figure 2 to enhance the bond performance between the FRP bars and the surrounding concrete. In addition, Figure 2 shows the tested CFRP-bars to illustrate the material's failure. Table 3 shows the details of the CFRP. All the

**Table 4.** Mix design proportion (kg/m<sup>3</sup>).

Cement	Silica fume	Super plasticizer	Lime	Gravel	Sand	Water
490	40	9.5	74.5	755	755	191

**Table 5.** SCC tests results.

Slump flue	V funnel	L box	Segregation ratio
T50 = 5.5 s Dmax = 65 cm	4 s	H2/H1 = 0.83	14%



T50 &amp; Dmax



L Box



V Funnel



Segregation

**Figure 3.** SCC tests.

FRP reinforcement used in this study was manufactured by LAMACO Inc.

### **Steel reinforcement**

Deformed steel bars (14 and 12 mm diameter) were used for longitudinal and shear reinforcement, respectively. Based on the test results, the yield stress and modulus of elasticity were 450 MPa and 200 GPa, respectively. Additionally, 12 mm-diameter steel bars were used to fabricate the stirrups for the control beam. The yield stress and modulus of elasticity were 550 MPa and 200 GPa, respectively.

### **Concrete**

The beam specimens were constructed using self-compacting concrete (SCC) provided by a tested mix design and cast in place in the concrete laboratory. The concrete used was high strength concrete (HSC) with a target compressive strength of 95 MPa after 28 days. The mix design properties and SCC tests results are shown in Tables 4, 5 and Figure 3. 36 concrete cubic samples of 100 x 100 mm were cast and cured under the same conditions as the test beams. Eight cubic samples were tested in compression after 28 days; four cubic samples were tested in compression on



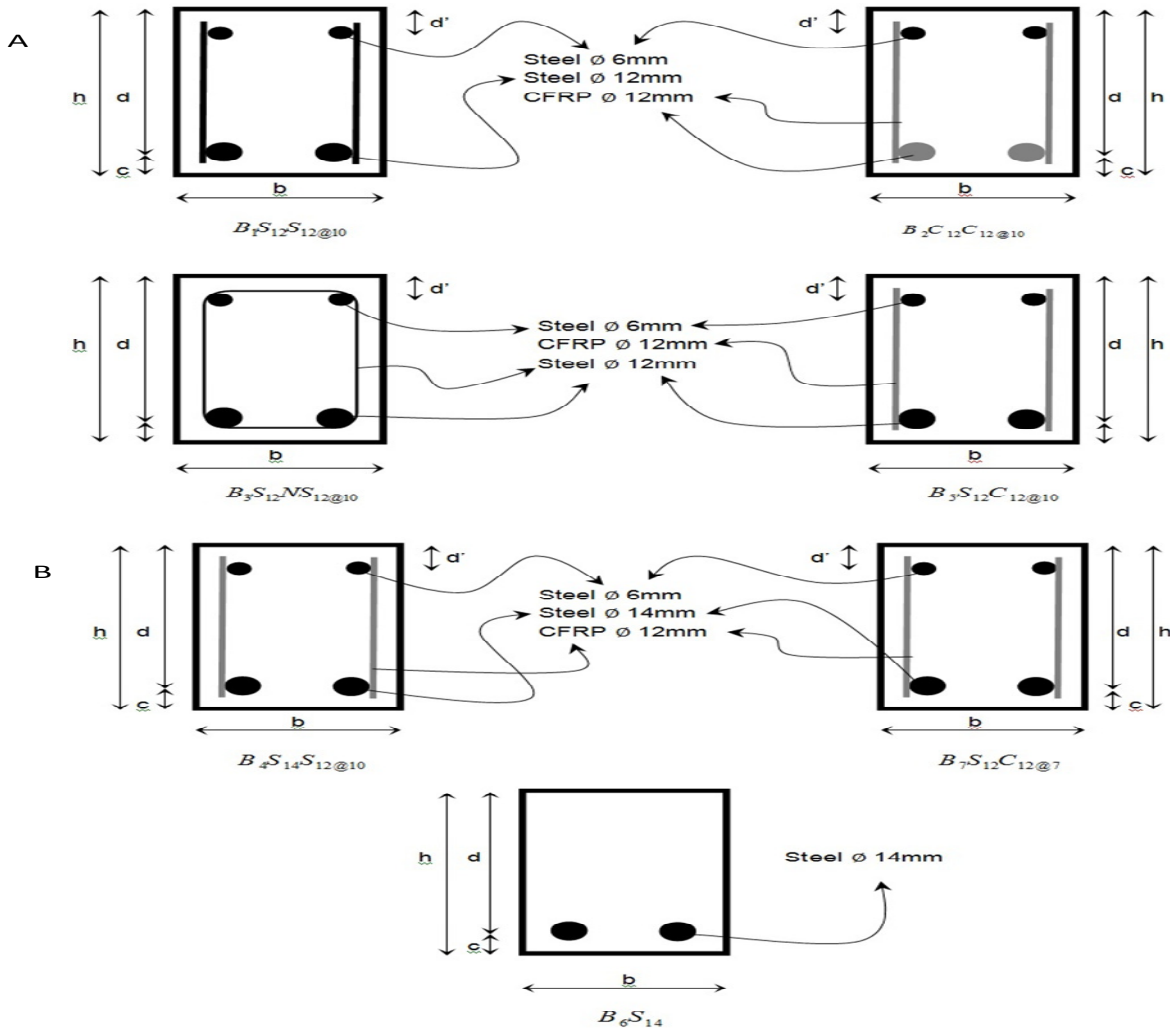


**Figure 4.** A, Group one beams. \* $h = 250$  mm,  $d = 220$  mm, cover = 30 mm,  $d' = 35$  mm, length of shear reinforcement = 230 mm. B, Group one beams. \*  $h = 250$  mm,  $d = 220$  mm, cover = 30 mm,  $d' = 35$  mm, length of shear reinforcement = 230 mm.

the day of beam testing and the stress-strain relationship was measured; four cylinders were tested in tension by performing the split cylinder test on the day of beam testing. The average compression strength ranged from 93.5 to 98.5 MPa and the average tensile strength ranged from 4.602 to 4.631 MPa. The average modulus of elasticity measured 34.838 GPa.

**Specimens**

In this study, seven beams were made and tested; the test specimens had a total length of 3005 mm with a clear span of 2850 mm. The overall cross section measured 250 mm deep and 200 mm wide. The shear span of the test specimens was kept constant at 925 mm. In addition, all beams were provided with different longitudinal reinforcement. Group one: the control beam was reinforced with a longitudinal steel bar (12 mm) and a normal steel stirrup (12 mm), its name was  $B_3 S_{12} NS_{12@10}$ . Two beams were reinforced with No. 12 steel longitudinal reinforcement with different shear reinforcement bars; the beam called  $B_1 S_{12} S_{12@10}$  used No. 12

steel shear bars equally spaced at 100 mm, which represents  $d/2$ , and the beam named  $B_5 S_{12} C_{12@10}$  used No. 12 CFRP shear bars with the spacing of the replacement equal to 100 mm, which represents  $d/2$ . One beam used No.12 CFRP longitudinal reinforcement with No.12 CFRP shear reinforcement. The shear bars were spaced at 100 mm. The beam was named  $B_2 C_{12} C_{12@10}$ . The group one beams and schematic beams in mould are shown in Figure 4a, Figure 5 and Table 6. Group two: Three beams were reinforced with No.14 steel longitudinal reinforcement. Two beams in this group used CFRP bars as shear reinforcement:  $B_4 S_{14} S_{12@10}$  with an equal spacing of 100 mm and  $B_7 S_{12} C_{12@7}$  with an equal spacing of 70 mm, which represents  $d/3$ . The third beam was  $B_6 S_{14}$  without shear reinforcement or stirrups. The group two beams and schematic beams in mould are shown in Figures 4b, 5 and Table 6. In addition, Figure 6 shows how to tie and install the shear reinforcement bars to the main reinforcement bars.

As Figure 6 shows, during casting, to determine the compressive



Figure 5. Beams in moulds to cast.

Table 6. Details of SCC reinforced beams.

Group name	Beams symbol	Main reinforcement bar	Shear reinforcement bar	Shear reinforcement spacing (cm)
One	$B_1S_{12}S_{12@10}$	Steel $\varnothing$ 12	Steel $\varnothing$ 12	10
	$B_2C_{12}C_{12@10}$	CFRP $\varnothing$ 12	CFRP $\varnothing$ 12	10
	$B_3S_{12}NS_{12@10}$	Steel $\varnothing$ 12	Steel $\varnothing$ 12	10
	$B_5S_{12}C_{12@10}$	Steel $\varnothing$ 12	CFRP $\varnothing$ 12	10
Two	$B_4S_{14}S_{12@10}$	Steel $\varnothing$ 14	Steel $\varnothing$ 12	10
	$B_6S_{14}$	Steel $\varnothing$ 14	-	-
	$B_7S_{12}C_{12@7}$	Steel $\varnothing$ 12	CFRP $\varnothing$ 12	7

strength of the concrete beams, four samples for each beam were taken from the concrete prepared. The beams were removed from the moulds after three days, and were kept in the laboratory under wet sacks and large plastic bags for 28 days. After this period, the samples were stored in the laboratory. After 166 days, the beams were tested.

#### Test setup and procedure

To monitor the behaviour of the tested beams, different instruments were used to measure the deflection at the mid-span, strains in the shear and flexural reinforcement, strains in concrete and crack widths. The instrumentation of the beams included linear variable displacement transducers (LVDTs) for deflection, electrical strain gauges for strain measurements. In addition, demec gauges of 200 mm length for measuring the neutral axis were used. Additionally, the locations of the strain gauges attached to the longitudinal flexural reinforcement and shear reinforcements are detailed in Figure 7 for all tested beams. As shown in Figure 7, the beams

were located over a simply supported clear span of 2850 mm. For all specimens the load was automatically applied using one actuator of 600 kN capacity with a load controlled rate of 6 kN/min, the load was applied at a displacement controlled rate of 0.2 mm/min to overcome any accidental problems of sudden and brittle shear failure. During the test, the loading was stopped at each 10 kN until 80% of the calculated design load; at each stop the crack widths and demecs were measured. The first initial crack widths were measured using a hand-held microscope with a magnifying power of 50X. The applied loads, deflection, and strains in reinforcement were recorded using a data acquisition system connected to a computer.

## RESULTS AND DISCUSSION

### Equations

According to created beams, CFRP and steel bars were



Figure 6. Taking samples to determine the compressive strength, modulus of elasticity, tensile strength and flexural strength.

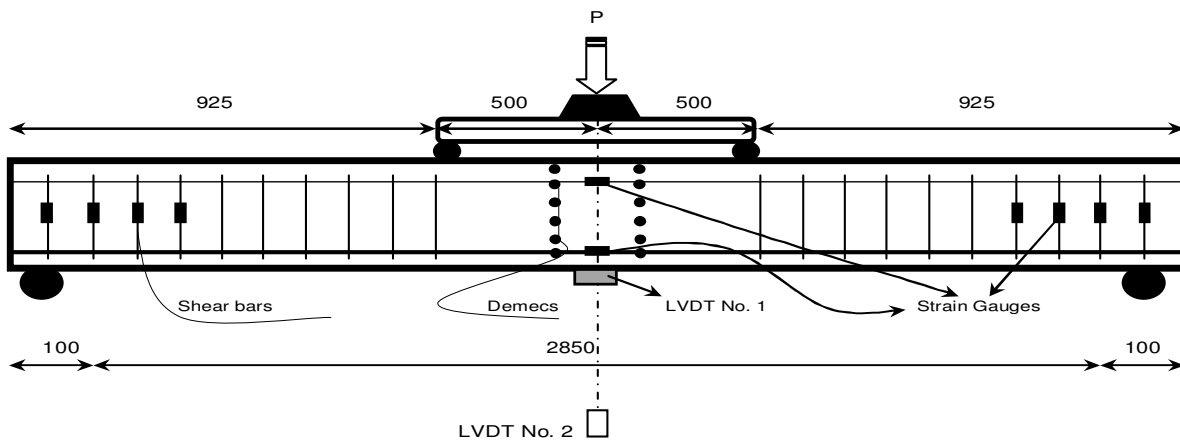


Figure 7. Schematic shape.

used as main and shear reinforcement bars. Therefore, to predict and determine the shear and flexural capacity of those beams and compare them with experimental results, ACI 440 (Guide for the Design and Construction of Structural Concrete Reinforced with FRP Bars) and ACI 318 (Building Code Requirements for Structural Concrete and Commentary) are used.

**Calculate nominal moment for  $B_2C_{12}C_{12@10}$  according to ACI 440**

$$f_f = \left( \sqrt{\frac{(0.003E_f)^2}{4} + \frac{0.85\beta_f f'_c}{\rho_f}} - 0.0015E_f \right)$$

$$M_n = \rho_f f_f \left( 1 - 0.59 \frac{\rho_f f_f}{f'_c} \right) b d^2 \quad (1)$$

**Calculate nominal moment for  $B_1S_{12}S_{12@10}$  -**

$B_3S_{12}NS_{12@10}$  -  $B_4S_{14}S_{12@10}$  -  $B_5S_{12}C_{12@10}$  -  $B_7S_{12}C_{12@7}$   
**according to ACI 318**

$$a = \frac{A_s f_y}{0.85 f'_c b} \quad M_n = A_s f_y \left( d - \frac{a}{2} \right) \quad (2)$$

**Calculate nominal shear strength for  $B_6S_{14}$  according to ACI 318**

$$V_c = \frac{\sqrt{f'_c}}{8} b d \quad (3)$$

**Table 7.** Design parameters properties.

Beams	Designed moment (kN.m)	Designed vertical load (kN)	Computed $\rho$	Computed $\rho_f$	Computed $\rho$ (min)	Computed $\rho_f$ (min)	Computed $\rho_b$	Computed $\rho_{fb}$
$B_1S_{12}S_{12@10}$	22.45		0.0026		0.0025		0.041	
$B_2C_{12}C_{12@10}$	74			0.0025		0.0014		0.002
$B_3S_{12}NS_{12@10}$	22.45		0.0026		0.0025		0.041	
$B_4S_{14}S_{12@10}$	30.36		0.0035		0.0025		0.041	
$B_5S_{12}C_{12@10}$	22.45		0.0026		0.0025		0.041	
$B_6S_{14}$		95.8	0.0035		0.0025		0.041	
$B_7S_{12}C_{12@7}$	30.36		0.0035		0.0025		0.041	

**Table 8.** Details of ultimate-nominal moment in group one.

Beams	Mn (KN.m)	Mu (KN.m)	Mu/Mn
$B_1S_{12}S_{12@10}$	22.45	32.14	1.43
$B_2C_{12}C_{12@10}$	74	61.32	0.83
$B_3S_{12}NS_{12@10}$	22.45	32.82	1.46
$B_5S_{12}C_{12@10}$	22.45	31.26	1.39

Calculate  $\rho_b$  and  $\rho_{min}$  according to ACI 318 and ACI 440

$$\rho_{min} = \frac{1.4}{f_y} \quad (4)$$

$$\rho_b = \left( \frac{0.85\beta_1 f'_c}{f_{fu}} \right) \left( \frac{600}{600 + f_y} \right) \quad (5)$$

$$f_{fu} = C_E f_{fu}^* \quad (6)$$

$$\rho_{fb} = \left( \frac{0.85\beta_1 f'_c}{f_{fu}} \right) \left( \frac{E_f \epsilon_{cu}}{E_f \epsilon_{cu} + f_{fu}} \right) \quad (7)$$

All details of nominal moments are shown in Table 7.

### Comparison of ultimate load and moment of beams

As mentioned earlier, seven beams were tested. After investigation of group one beams and, especially

$B_1S_{12}S_{12@10}$ ,  $B_3S_{12}NS_{12@10}$  and  $B_5S_{12}C_{12@10}$ , it has been demonstrated that the ultimate moment in these beams are close together and the ratio of UM/DM in all are bigger than 1.0, with the lowest being 1.39 and the largest being 1.46. Only in the beam called  $B_2C_{12}C_{12@10}$ , in which CFRP-bars were used as the main and shear reinforcement bars was the  $\frac{M_u}{M_n}$  lower than 1. The reason

for this can be attributed to the high tensile strength of CFRP (ACI 440, 2006). The flexural zone had good resistance and the cracks shifted to the shear zone. With continued loading, the shear zone could not accommodate more cracks and the beams suddenly broke in the shear area. In addition, in the beams that used CFRP bars as the main reinforcement, the failure is brittle and in the shear area (ACI 440, 2006). During loading of  $B_2C_{12}C_{12@10}$ , the cracks have gone to be shear crack and, finally, in the shear area of the main bars, brittle failure has been observed. This could be prevented by reducing the distance of the CFRP shear reinforcement bars, for example instead of  $d/2$ , choose  $d/3$  or  $d/4$ . The details are shown in Table 8. In the group two beams, the ratio of  $\frac{M_u}{M_n}$  was bigger than 1.5 in which

the largest was 1.77 for  $B_7S_{12}C_{12@7}$ . However, it is necessary to explain that shear failure was seen in  $B_6S_{14}$ , which did not have shear reinforcement bars.



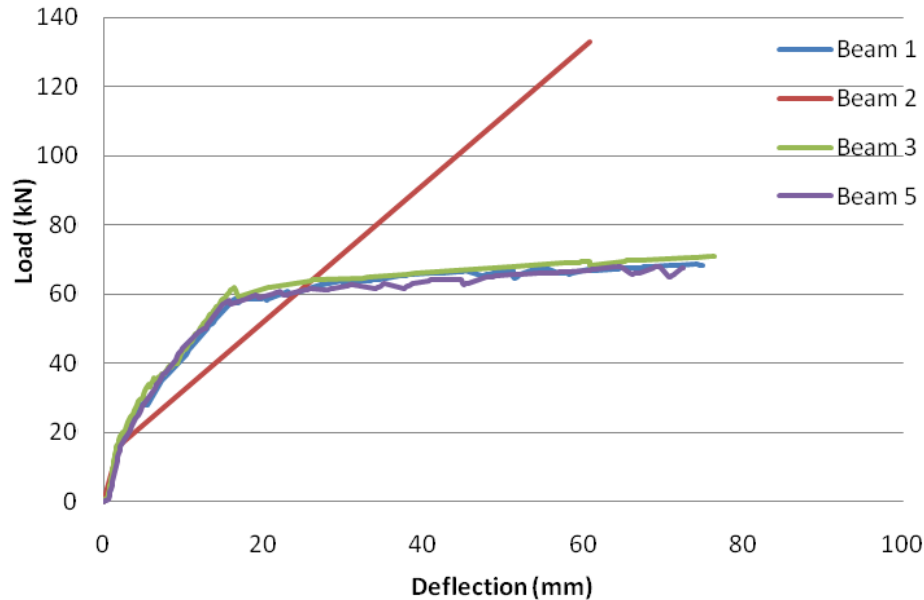


Figure 8. Group one load and deflection curve.

Table 9. Details of ultimate- nominal load and moments in group two.

Beams	$M_n$ (kN.m)	$M_u$ (kN.m)	$M_u/M_n$	$V_c$ (kN)	$V_u$ (kN)	$V_u/V_c$
$B_4S_{14}S_{12@10}$	30.36	46.60	1.53			
$B_6S_{14}$				95.8	98.76	1.03
$B_7S_{12}C_{12@7}$	30.36	54.42	1.77			

Although the final rupture was a kind of shear failure and brittle, however, being horizontal, the graph in Figure 8 at 90 kN loading shows that the concrete has shown good shear resistance and partly succeeded to control the shear cracks. Furthermore, the main bars reached plastic behaviour; shear failure occurred after continued loading (Faisal et al., 1994). This shear crack could be observed within 10 min before the collapse. Details are shown in Table 9. According to Table 8 and 9, it can be said that in those beams in which their  $\rho$  is 50% to 85%  $\rho_b$ , the usage of CFRP bars as shear reinforcement can be a good alternative for the traditional stirrups.

#### Comparison of load-deflection and investigation of modes of failure

In group one and in the control beam,  $B_3S_{12}NS_{12@10}$  from 0 to 20 kN the beam behaviour was linear and un-cracked. From this point the main bars showed elastic behaviour. The yield point was 61 kN. From 0 to 61 kN, a small deflection (20 mm) can be observed which with increasing loading from 61 to 70 kN, a large deflection

was seen (60 mm) and the beam showed plastic behaviour. In  $B_1S_{12}S_{12@10}$  it can be said that the behaviour of this beam is 90% similar to  $B_3S_{12}NS_{12@10}$ . The yield point is 59 kN with a recorded deflection of 17 mm. With a loading of 70 kN, the deflection increased to 80 mm. Beauvoir in  $B_5S_{12}C_{12@10}$  is also the same as  $B_1S_{12}S_{12@10}$ , the only difference being the initial deflection. In  $B_1S_{12}S_{12@10}$  has been seen less initial deflection compared with  $B_5S_{12}C_{12@10}$ , however, the difference was minimal. The behaviour of the beams with FRP as reinforcement bars is totally different from the RC beams with steel bars. In  $B_2C_{12}C_{12@10}$  has been used CFRP-bars for the main reinforcement bars and the behaviour of the beams was linear. As predicted, there is not a yield point and after reaching the failure point, the bars will rupture. In this beam, the failure point was at 132.6 kN with 60 mm deflection. It can be said that the higher ultimate load with less deflection in reinforced FRP beams in comparison with the similar RC beams reinforced with steel is noteworthy. In addition, clearly the disadvantage of FRP RC beams is the brittle failure (ACI 440, 2006). In group

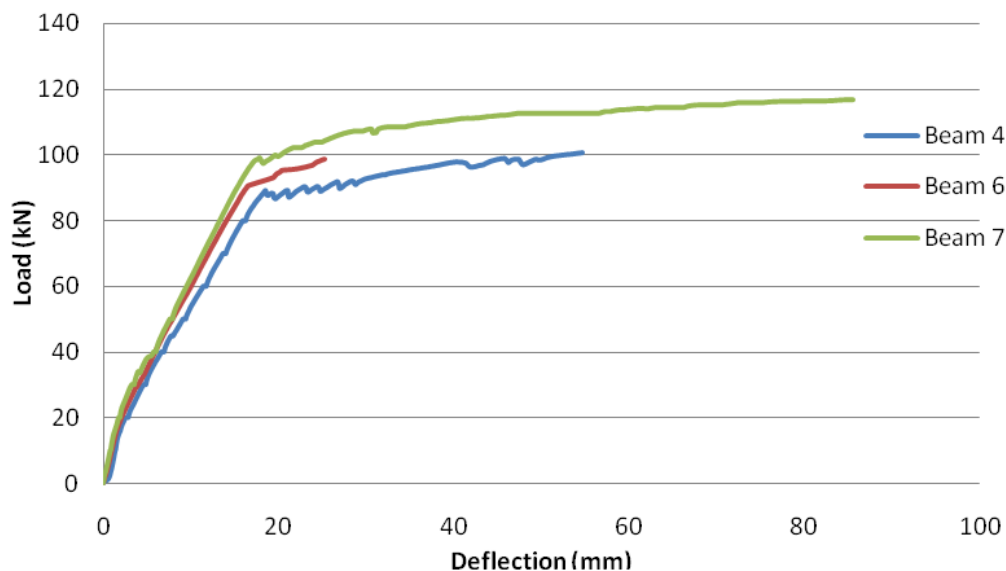


Figure 9. Group two load and deflection curve.

two and in  $B_4S_{14}S_{12@10}$ , the yield point started at 84 kN and continued to 105 kN with 55 mm deflection. Regarding the use of CFRP shear reinforcement, it can be said that  $B_4S_{14}S_{12@10}$  has shown good behaviour that is comparable to that of a normal beam and from Figure 9 it can be seen that the behaviour of the shear reinforcement bars is similar to normal stirrups; this beam failed in the flexural zone.

In  $B_6S_{14}$ , which had two main bars without shear reinforcement bars, the failure happened in the shear zone as predicted. As is clear from Figure 9, until 90 kN the 'load-deflection' curves are linear and after 90 kN to 95. It can be identified that the main bar partly yielded due to the good shear strength of concrete. In high strength concrete beams without shear reinforcement bars, the ratio of  $\frac{\alpha}{d}$  is very critical, so that if  $4 < \frac{\alpha}{d} < 6$ , the mode of failure is shear-flexural (Faisal et al., 1994). Also, in terms of ultimate capacity,  $B_6S_{14}$  and  $B_4S_{14}S_{12@10}$  are very close, however, it has been demonstrated many differences in deflection. At 90 kN the deflections are similar, 20 mm, but from this point to the ultimate load in  $B_6S_{14}$  the deflection increased to 27 mm, whereas for  $B_4S_{14}S_{12@10}$  the deflection increased to 80 mm. From a

comparison of  $B_4S_{14}S_{12@10}$  and  $B_6S_{14}$  it can be said that there is no significant difference in ultimate capacity, however, the usage of shear reinforcement in  $B_4S_{14}S_{12@10}$  is used to avoid brittle rupture in the shear zone. The manufacture of  $B_7S_{12}C_{12@7}$  was

similar to  $B_4S_{14}S_{12@10}$  but with a difference in the distance of replacement CFRP shear reinforcement; in  $B_4S_{14}S_{12@10}$  it was  $\frac{d}{2}$  and in  $B_7S_{12}C_{12@7}$  it was  $\frac{d}{3}$ . The yield point in  $B_7S_{12}C_{12@7}$  was at 98 kN with 18 mm deflection. With continued loading, until 116.5 kN, the deflection increased to 85 mm due to the good behaviour of the beams which shows that usage of shear reinforcement bars can prevent shear failure.

### Investigation of flexural and shear cracks

From the investigation and comparison of the mode of cracks it can be said that in all beams the first crack appeared in the flexural zone with the load of first crack being between 16.3 and 20 kN. With increasing loading, more flexural cracks were observed and at 40 to 60 % of the ultimate load these cracks emerged in the shear zone. Group one: According to Table 10, and from analysis of the crack modes in Figure 10 and comparison of  $B_3S_{12}NS_{12@10}$ ,  $B_1S_{12}S_{12@10}$  and  $B_5S_{12}C_{12@10}$ , it is understood that shear reinforcement bars can be an alternative instead of stirrups, as the mode of cracks in these beams are very similar to each other. In  $B_2C_{12}C_{12@10}$  good crack extension was seen in the whole beam, however, the crack width was larger (Chitsazan et al., 2010). Although the cracks were satisfactory before rupture, for reasons that were investigated previously the failure was brittle and in the shear area. Group two: Regarding the lack of shear reinforcement bars in  $B_6S_{14}$ , less total cracks were recorded. In  $B_4S_{14}S_{12@10}$  and  $B_7S_{12}C_{12@7}$  the type of

**Table 10.** Details of crack widths and load of first cracks.

Beams	Load of first crack (kN)	Width of first crack (mm)	FCL/UL	Average load of first crack (kN)	Average of FCL/UL
$B_1S_{12}S_{12@10}$	20	0.08	0.28		
$B_2C_{12}C_{12@10}$	17.35	0.12	0.13		
$B_3S_{12}NS_{12@10}$	19.2	0.08	0.27		
$B_4S_{14}S_{12@10}$	16.3	0.04	0.16	18.66	0.21
$B_5S_{12}C_{12@10}$	17.8	0.08	0.26		
$B_6S_{14}$	20	0.06	0.20		
$B_7S_{12}C_{12@7}$	20	0.02	0.17		

\*FCL is first crack loading, UL is ultimate load.

cracking was similar but in  $B_7S_{12}C_{12@7}$ , in which the distance of the replaced shear reinforcement bars were closer than in  $B_4S_{14}S_{12@10}$ , more cracking was seen. Table 10 and Figure 10 show the mode of cracks, details of crack width and load of first cracks.

### Cracks simulation

#### Investigation of neutral axis of beams

Group one: at 70% of the ultimate load or 30 kN according to observation we can say that the neutral axis in  $B_3S_{12}NS_{12@10}$  was located almost in the middle and at 119 mm from the bottom. In  $B_1S_{12}S_{12@10}$  the neutral axis was 179 mm from the bottom. In  $B_5S_{12}C_{12@10}$  similar to  $B_1S_{12}S_{12@10}$  the neutral axis was located above the neutral axis in  $B_3S_{12}NS_{12@10}$  with little difference, the position of the neutral axis in  $B_5S_{12}C_{12@10}$  was 173 mm. In  $B_2C_{12}C_{12@10}$ , which used CFRP bars as the main reinforcement, the neutral axis moved significantly higher and is located at 191 mm. Of course, this behaviour has been reported in previous studies (Chitsazan et al., 2010) (Figure 11). Group two: in  $B_6S_{14}$  at 40 kN the neutral axis was located in the highest recorded position in this category – at 185 mm. Obviously, if CFRP shear reinforcement was used, the position of the neutral axis would be located lower to use more of the compressive capacity of the concrete. From a comparison of  $B_4S_{14}S_{12@10}$  and  $B_7S_{12}C_{12@7}$  in Figure 12, it has been recognized that if the distance of placing CFRP shear reinforcement is closer, the position of the neutral axis will be lower. At 40 kN loading, the position of the neutral axis in  $B_4S_{14}S_{12@10}$  and  $B_7S_{12}C_{12@7}$  was 161 and 148 mm, respectively. In addition, at the same load and with 40 kN loading, the position of the neutral axis in

$B_7S_{12}C_{12@7}$  was lower than  $B_3S_{12}NS_{12@10}$ .

### CONCLUSION

From the experimental results in this research the following conclusions can be drawn: The most important point arising from the results in this research is that the CFRP shear reinforcement bars can be considered as an attractive alternative instead of normal stirrups in RC beams where their  $\rho$  are 50 to 85%  $\rho_b$ . The beams reinforced with FRP have greater capacity with less deflection compared to the concrete beams reinforced with steel. In addition, there is no significant difference in the ultimate capacity in the beams cast with high strength concrete and the RC beams with shear reinforcement and the RC beams without shear reinforcement, however, using shear reinforcement will avoid brittle rupture and the beams will exhibit more deflection. In high strength concrete beams without shear reinforcement bars, the ratio of  $\frac{\alpha}{d}$  is very critical and if  $4 < \frac{\alpha}{d} < 6$ , the mode of failure is shear-flexural. The beams reinforced with CFRP have good crack extension in the whole beam, however, the width of cracks is larger than the RC beams with steel. By decreasing the distance of the replacement CFRP shear reinforcement bars, the number of cracks increase but the width of the crack is narrower.

### CODE NOTATION

$a$  = depth of equivalent rectangular stress block;  $b$  = width of rectangular cross section;  $d$  = distance from extreme compression fibre to centroid of tension reinforcement;  $A_f$  = area of FRP reinforcement;  $A_s$  =





Group two:

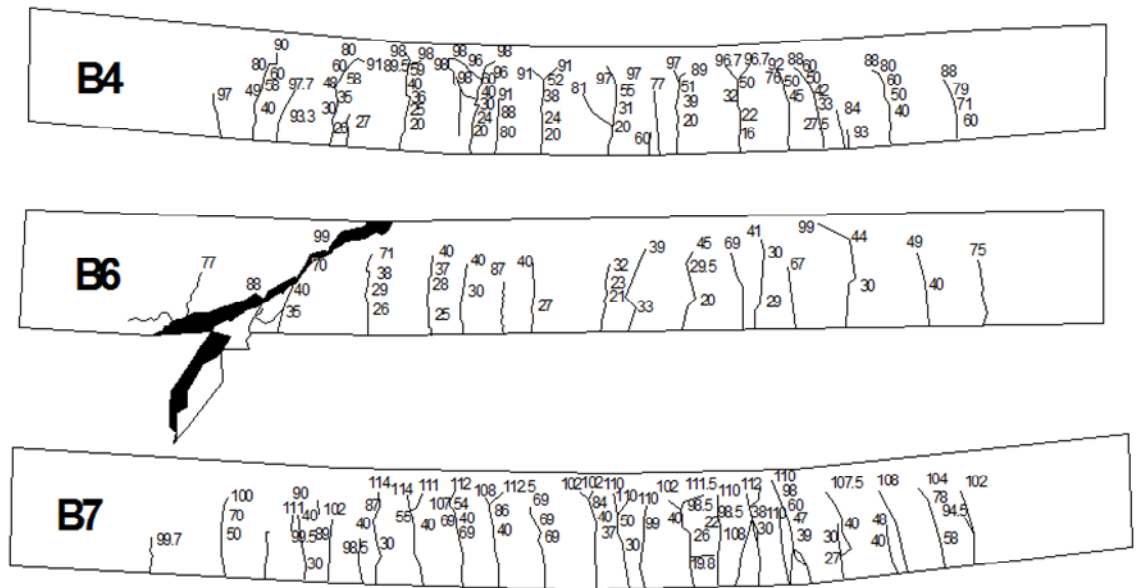


Figure 10. Details of mode of cracks.

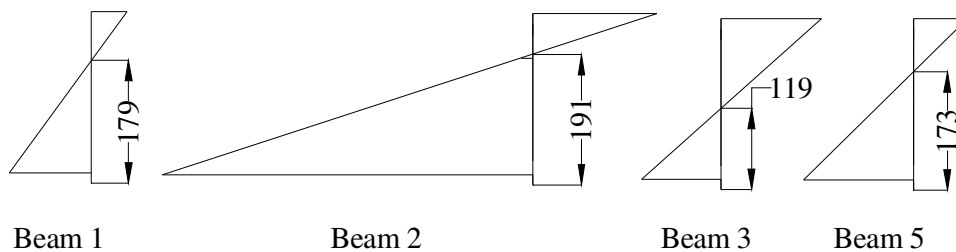


Figure 11. Group one neutral axis (mm).

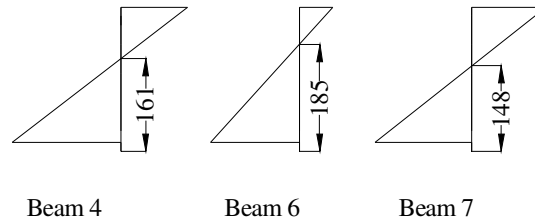


Figure 12. Group two neutral axis (mm).

area of tension steel reinforcement;  $E_f$  = design or guaranteed modulus of elasticity of FRP defined as mean modulus of sample of test specimens;  $f_c'$  = specified compressive strength of concrete;  $f_{cu}$  = characteristic cube strength of concrete;  $f_f$  = stress in FRP reinforcement in tension;  $f_{fu}^*$  = guaranteed tensile strength of FRP bar;  $f_{fu}$  = design tensile strength of FRP, considering reductions for service environment;  $C_E$  = environmental reduction factor for various fibre type and exposure conditions for CFRP and used condition was 1.0;  $f_y$  = specified yield stress of nonprestressed steel reinforcement;  $M_n$  = nominal moment capacity;  $M_u$  = factored moment at section;  $V_c$  = nominal shear strength provided by concrete;  $V_u$  = factored shear force at section;  $\rho_f$  = FRP reinforcement ratio;  $\rho_{fb}$  = FRP reinforcement ratio producing balanced strain conditions;  $\rho_b$  = steel reinforcement ratio producing balanced strain conditions;  $\rho_{min}$  = minimum reinforcement ratio for steel;  $\alpha$  = shear span, distance from support to the first concentrated load;  $\beta_1$  = factor taken as 0.85 for concrete strength;  $f_c'$  up to and including 28 MPa. For strength above 28 MPa, this factor is reduced continuously at a rate of 0.05 per each 7 MPa of strength in excess of 28 MPa but is not taken less than 0.65.

## REFERENCES

- ACI 440.3R-04 (2004). Guide test methods for fiber-reinforced polymers (FRPs) for reinforcing or strengthening concrete structures. ACI, Farmington Hills, MI, USA.
- ACI Committee 318 (1999). Building code requirements for structural concrete (ACI 318-99) and commentary(318R-99). ACI, Farmington Hills, Mich.
- ACI Committee 440 (2006). Guide for the design and construction of concrete reinforced with FRP bars (ACI440.1R-06). ACI, Farmington Hills, Mich. Ali MSM, Oehlers DJ, Griffith MC, Seracinob R (2008). Interfacial stress transfer of near surface-mounted FRP-to-concrete joints. Eng. Struc. 30(7): 1861–1868.
- AIMusallam TH, Al-Salloum YA, Alsayed SH, Amjad MA (1997). Behavior of concrete beams doubly reinforced by FRP bars. Proceedings of the third international symposium on non-metallic (FRP) reinforcement for concrete structures (FRPRCS-3), Japan, 2: 471-478.
- Alsayed SH (1998). Flexural behaviour of concrete beams reinforced with GFRP bars. Cem. Concr. Compos. 20(1): 1-11.
- ASTM D618-61 (1995). Standard practice for conditioning plastics and electrical insulating materials for testing. Annual Book of ASTM Standards, vol. 8.01. Philadelphia, PA: American Society for Testing and Materials.
- Badawi M, soudki K (2009). Flexural strengthening of RC beams with prestressed NSM CFRP rods – Experimental and analytical investigation. Cons. Buil. Mater., 23(10): 3292-3300.
- Barros JAO, Fortes AS (2005). Flexural strengthening of concrete beams with CFRP laminates bonded into slits, Cem. Conc. Compo., 27(4): 471-480.
- Blaschko M, Zilch K (1999). Rehabilitation of concrete structures with strips glued into slits. Proceedings of the 12th Int. Conference on Composite Materials, Paris.
- Chitsazan I, Kobraei M, Zamin Jumaat M, Shafigh P (2010). An experimental study on the flexural behavior of FRP RC beams and a comparison of the ultimate moment capacity with ACI, J. Civ. Eng. Cons. Tech., 1(2): 27-42.
- Ei-Hacha R, Rizkalla SH (2004). Near-surface-mounted fiber-reinforced polymer reinforcements for flexural strengthening of concrete structures. Stru. J., 101 (5): 717-726.
- Faisal FW, Samir AA, Ghazi SH (1994). Shear behavior of reinforced high-strength concrete beams without shear reinforcement. Eng. J. Qatar Univ., 7: 91-113.
- Islam AKM (2009). Effective methods of using CFRP bars in shear strengthening of concrete girders. Eng. Stru., 31(3): 709-714.
- Lorenzis DL, Nanni A (2002). Bond between near-surface mounted FRP rods and concrete in structural strengthening, ACI Stru. J., 99 (2): 123-133.
- Nanni A (1999). Composites: Coming on Strong, Con. Constr. 44(1): 120-124.
- Novidis D, Pantazopoulou SJ, Tentolouris E (2007). Experimental study of bond of NSM-FRP reinforcement. Cons. Buil. Mater., 21(8): 1760-1770.
- Rizzo A, De Lorenzis L (2009). Behavior and capacity of RC beams strengthened in shear with NSM FRP reinforcement. Cons. Buil. Mater., 23 (4): 1555-1567.
- Thériault M, Benmokrane B (1998). Effects of FRP reinforcement ratio and concrete strength on flexural behavior of concrete beams. J. Compo. Const. 2(1): 7-16.
- Tureyen AK, Frosch RJ (2002). Shear tests of FRP-reinforced concrete beams without stirrups. ACI Struct. J. 99(4): 427-434.
- Wang B, Teng JG, Lorenzis LD, Zhou LM, Ou J, Jin W, Lau KT (2009). Strain monitoring of RC members strengthened with smart NSM FRP bars. Cons. Buil. Mater. 23(4): 1698-1711.
- Yang J, Wu YF (2007). Interfacial stresses of FRP strengthened concrete beams: Effect of shear deformation, Compo. Struct., 80(3): 343-351.
- Yost JR, Goodspeed CH, Schmeckpeper ER (2001). Flexural performance of concrete beams reinforced with grids. J. Compo. Constr., 5(1): 18-25.FRP.